Supplementary Material (ESI) for New Journal of Chemistry

Synthesis of 3- and 5-formyl-4-phenyl-1*H*-pyrazoles: promising head units for the generation of asymmetric imine ligands and polynuclear complexes

Juan Olguín[a] and Sally Brooker*[a]

Supporting information

Table S1. Crystal structure determination details for the compounds **14**, **19** and complex $[Fe^{II}(Ni^{II}L^2)_3](BF_4)_2 \cdot 1.25MeCN \cdot 1.25MeOH \cdot Et_2O$.

	Compound **14**	Compound **19**	**$[Fe(NiL^2)_3](BF_4)_2 \cdot 1.25MeCN \cdot 1.25MeOH \cdot Et_2O$**
Identification code	jophpzes	jl185	jo456b
Empirical formula	$C_{18}H_{20}N_2O_5$	$C_{15}H_{16}N_2O_2$	$C_{85.75}H_{72.75}B_2F_8FeN_{19.25}Ni_3O_{2.25}$
Formula weight	344.36	256.30	1814.48
Temperature	89 K	88 K	89 K
Wavelength	0.71073 Å	0.71073 Å	0.71073 Å
Crystal system	Orthorhombic	Monoclinic	Triclinic
Space group	$P2_12_12_1$	$P2_1/c$	P-1
Unit cell dimensions	a = 8.4741(5) Å α = 90°. b = 9.4806(5) Å β = 90°. c = 21.3093(14) Å γ = 90°.	a = 10.0556(5) Å α = 90°. b = 16.6586(9) Å β= 99.229(3)°. c = 7.7010(4) Å γ = 90°.	a = 12.5943(16) Å α = 84.789(7)°. b = 18.395(2) Å β = 85.699(7)°. c = 20.037(3) Å γ = 70.209(6)°.
Volume	1711.98(18) $Å^3$	1273.31(11) $Å^3$	4345.0(10) $Å^3$
Z	4	4	2
Density (calculated)	1.336 Mg/m^3	1.337 Mg/m^3	1.387 Mg/m^3
Absorption coefficient	0.098 mm^{-1}	0.090 mm^{-1}	0.879 mm^{-1}
F(000)	728	544	1864
Crystal size	0.43 x 0.37 x 0.35 mm^3	0.40 x 0.10 x 0.10 mm^3	0.40 x 0.20 x 0.18 mm^3
Theta range for data collection	1.91 to 30.15°.	2.95 to 26.43°.	1.02 to 27.49°.
Index ranges	$-11 \le h \le 11$, $-10 \le k \le 13$, $-30 \le l \le 29$	$-12 \le h \le 12$, $-19 \le k \le 20$, $-9 \le l \le 9$	$-16 \le h \le 16$, $-23 \le k \le 23$, $-25 \le l \le 26$
Reflections collected	12150	14804	55588
Independent reflections	5024 [R(int) = 0.0672]	2617 [R(int) = 0.0571]	19810 [R(int) = 0.0447]
Completeness to theta = 26.43°	99.6 %	99.7 %	99.2 %
Absorption correction	Semi-empirical from equivalents	Semi-empirical from equivalents	Semi-empirical from equivalents
Max. and min. transmission	0.7460 and 0.6207	0.9911 and 0.9649	0.8577 and 0.7038
Refinement method	Full-matrix least-squares on F^2	Full-matrix least-squares on F^2	Full-matrix least-squares on F^2
Data / restraints / parameters	5024 / 0 / 228	2617 / 0 / 173	19810 / 0 / 1146
Goodness-of-fit on F2	1.039	1.098	1.085
Final R indices [I>2sigma(I)]	R1 = 0.0624, wR2 = 0.1275	R1 = 0.0486, wR2 = 0.1147	R1 = 0.0743, wR2 = 0.1914
R indices (all data)	R1 = 0.0937, wR2 = 0.1438	R1 = 0.0665, wR2 = 0.1250	R1 = 0.0922, wR2 = 0.2040
Extinction coefficient		0.007(2)	
Flack parameter	0.2(13)†		
Largest diff. peak and hole	0.479 and -0.295 e.$Å^{-3}$	0.213 and -0.248 e.$Å^{-3}$	1.483 and -0.945 e.$Å^{-3}$

†as this is a light atom structure the absolute structure cannot be reliably determined.

Table S2. Selected bond lengths [Å] and angles [°] for complex $[Fe^{II}(Ni^{II}L^2)_3](BF_4)_2 \cdot 1.25MeCN \cdot 1.25MeOH \cdot Et_2O$.

Fe(1)-N(1)	2.119(3)
Fe(1)-N(13)	2.119(3)
Fe(1)-N(11)	2.119(4)
Fe(1)-N(5)	2.127(4)
Fe(1)-N(7)	2.127(3)
Fe(1)-N(17)	2.146(4)
Ni(2)-N(6)	1.824(4)
Ni(2)-N(2)	1.827(4)
Ni(2)-N(4)	1.843(4)
Ni(2)-N(3)	1.844(4)
Ni(3)-N(8)	1.821(4)
Ni(3)-N(12)	1.829(3)
Ni(3)-N(9)	1.845(4)
Ni(3)-N(10)	1.846(4)
Ni(4)-N(18)	1.824(3)
Ni(4)-N(14)	1.829(4)
Ni(4)-N(15)	1.837(4)
Ni(4)-N(16)	1.842(4)

N(1)-Fe(1)-N(13)	173.86(14)
N(1)-Fe(1)-N(11)	90.23(14)
N(13)-Fe(1)-N(11)	85.90(14)
N(1)-Fe(1)-N(5)	99.18(14)
N(13)-Fe(1)-N(5)	85.05(14)
N(11)-Fe(1)-N(5)	169.77(13)
N(1)-Fe(1)-N(7)	86.23(13)
N(13)-Fe(1)-N(7)	89.72(14)
N(11)-Fe(1)-N(7)	99.68(14)
N(5)-Fe(1)-N(7)	85.04(14)
N(1)-Fe(1)-N(17)	84.82(13)
N(13)-Fe(1)-N(17)	99.77(13)
N(11)-Fe(1)-N(17)	87.89(14)
N(5)-Fe(1)-N(17)	88.96(14)
N(7)-Fe(1)-N(17)	168.30(14)
N(6)-Ni(2)-N(2)	104.08(16)
N(6)-Ni(2)-N(4)	84.53(17)
N(2)-Ni(2)-N(4)	170.14(16)
N(6)-Ni(2)-N(3)	171.08(18)
N(2)-Ni(2)-N(3)	84.67(17)
N(4)-Ni(2)-N(3)	86.60(18)
N(8)-Ni(3)-N(12)	104.74(16)
N(8)-Ni(3)-N(9)	84.14(16)
N(12)-Ni(3)-N(9)	171.06(17)
N(8)-Ni(3)-N(10)	170.99(16)
N(12)-Ni(3)-N(10)	84.26(16)
N(9)-Ni(3)-N(10)	86.85(16)
N(18)-Ni(4)-N(14)	104.94(15)
N(18)-Ni(4)-N(15)	170.88(16)
N(14)-Ni(4)-N(15)	84.18(16)
N(18)-Ni(4)-N(16)	84.24(16)
N(14)-Ni(4)-N(16)	170.81(16)
N(15)-Ni(4)-N(16)	86.65(16)

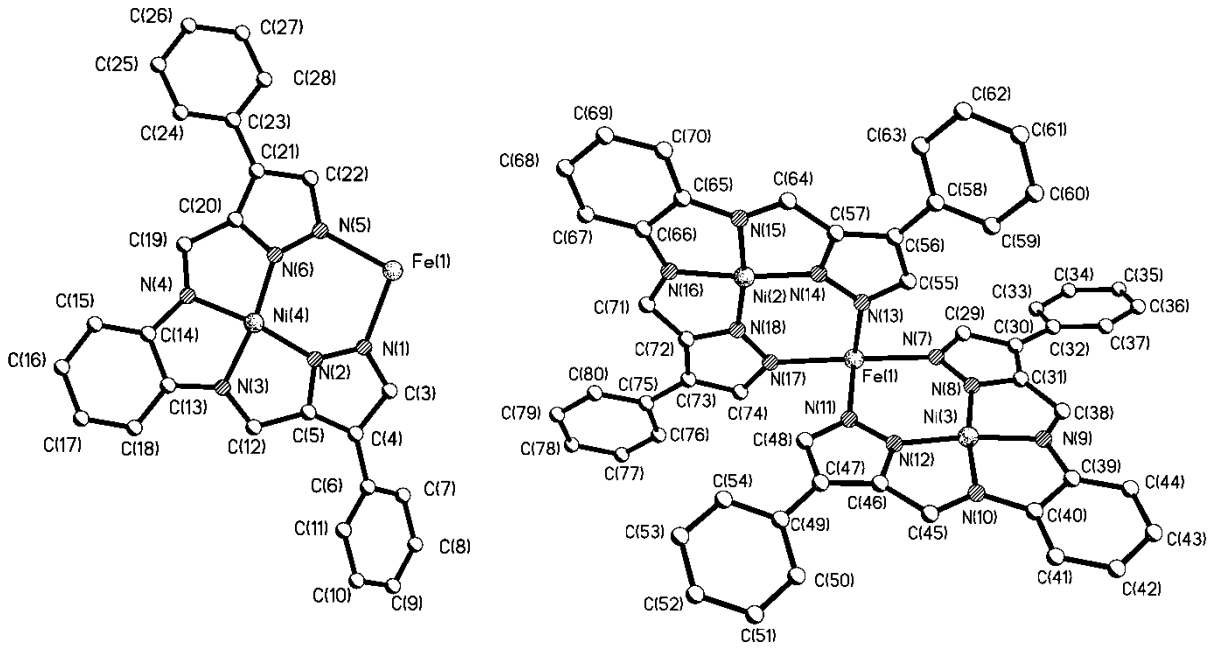

Figure S1. Numbering scheme for complex $[Fe^{II}(Ni^{II}L^2)_3](BF_4)_2 \cdot 1.25MeCN \cdot 1.25MeOH \cdot Et_2O$. N.B. these are NOT perspective views of the complex, rather one of the three 'complexes as a ligand' is shown on the LHS and the other two 'complexes as ligands' are shown on the right hand side; all three bind to one central iron centre.

Packing of N-protected monoaldehyde **19**

A detailed analysis of the crystal packing of this compound shows that the carbonyl group of each molecule interacts with the neighbouring molecules on each side of it in the stack as follows (Figure S2): (a) a π…π interaction with the pyrazole ring of the neighbouring molecule on one side (carbonyl C(4)'…pyrazole centroid 3.179 Å) (b) and a C-H…O interaction with the THP group of the molecule on the other side (carbonyl O(1)'…C(15)" 3.203(2) Å). As a consequence of the latter interaction the oxygen of the THP group makes a short contact with the carbon of the carbonyl group (O(2)"…C(4)' 3.155(2) Å). These intermolecular interactions lead to the formation of chains along the *c* axis (Figure S3).

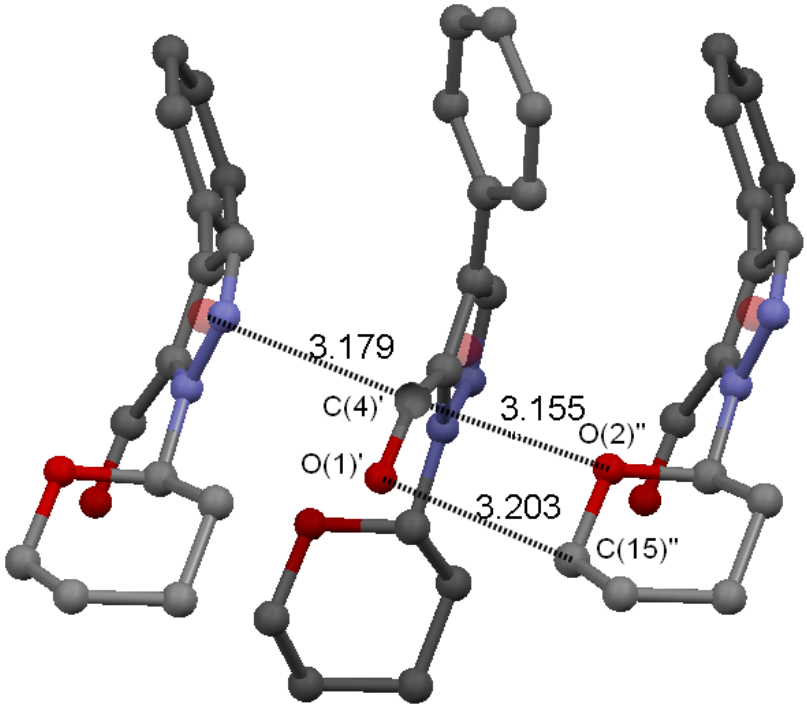

Figure S2. Ball and stick representation of the CH…π and CH…O interactions present between a adjacent molecules in the structure of N-protected monoaldehyde **19**.

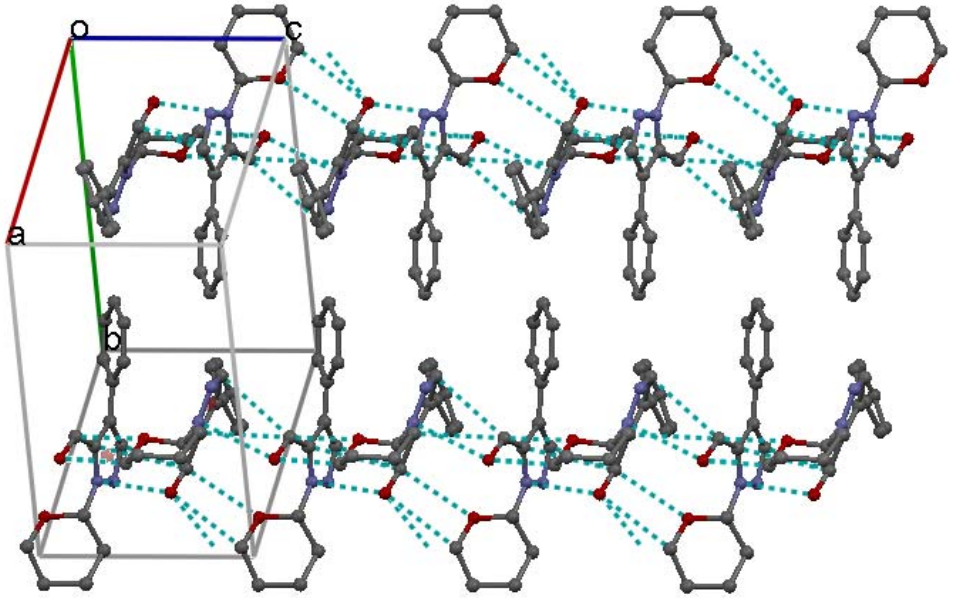

Figure S3. Ball and stick representation of two of the supramolecular chains that run along the *c* axis in the crystal lattice of N-protected monoaldehyde **19**.